Research Square

Preprints are preliminary reports that have not undergone peer review.
They should not be considered conclusive, used to inform clinical practice,
or referenced by the media as validated information.

Bilateral biomechanical alterations during side-cutting in patients with patellar tendinopathy

qiaoqiao wang
Peking University Third Hospital
lingjie chen
Peking University Third Hospital
yijing zhou
Peking University Third Hospital
si zhang
Peking University Third Hospital
shuang ren
Peking University Third Hospital
hongshi huang
huanghs@bjmu.edu.cn
Peking University Third Hospital

Research Article

Keywords: biomechanics, ground reaction force, patellar tendinopathy, side-cutting, statistical parametric mapping, tendon loading

Posted Date: November 13th, 2026

DOI: https://doi.org/10.21203/rs.3.rs-11356328/v1

License: This work is licensed under a Creative Commons Attribution 4.0 International License.
Read Full License

Additional Declarations: No competing interests reported.

Bilateral biomechanical alterations during side-cutting in patients with patellar tendinopathy

Qiao-qiao Wang[a,b,c,†], Ling-jie Chen[a,b,c,†], Yi-jing Zhou[a,b,c], Si Zhang[a,b,c], Shuang Ren[a,b,c,*], Hong-shi Huang[a,b,c,*]

a. Department of Sports Medicine, Peking University Third Hospital, Institute of Sports Medicine of Peking University, Beijing, China

b. Beijing Key Laboratory of Research and Translation for Drugs and Medical Devices in Precision Diagnosis and Treatment of Sports Injuries, Beijing, China

c. Engineering Research Center of Sports Trauma Treatment Technology and Devices, Ministry of Education, Beijing, China

† Qiao-qiao Wang and Ling-jie Chen contributed equally to this work and are co-first authors.

* Corresponding authors: Shuang Ren, Department of Sports Medicine, Peking University Third Hospital, 49 North Garden Road, Haidian District, Beijing 100191, China. Email: xixishuang123@126.com. Tel: +86-176-1025-2992. Hong-shi Huang, Department of Sports Medicine, Peking University Third Hospital, 49 North Garden Road, Haidian District, Beijing 100191, China. Email: huanghs@bjmu.edu.cn. Tel: +86-10-8226-7567.

Bilateral biomechanical alterations during side-cutting in patients with patellar tendinopathy

Abstract

Background: Biomechanical research in patellar tendinopathy (PT) has focused on sagittal-plane loading during jumping and landing; how patients with PT perform side-cutting is unknown. This study compared hip and knee biomechanics and estimated patellar tendon force during side-cutting among the affected (AL) and unaffected (UL) legs of patients with PT and the dominant leg (DL) of healthy controls.

Methods: In this cross-sectional laboratory study, 30 patients with PT and 30 demographically matched healthy controls performed anticipated 45° side-cuts. Stance-phase ground reaction forces (GRF), three-dimensional hip and knee angles and moments, estimated patellar tendon force, and movement-strategy metrics were compared using one-dimensional statistical parametric mapping (SPM) and linear mixed models.

Results: Versus the DL, both PT legs showed greater hip internal rotation and knee varus across most of stance, smaller mid-stance hip internal rotation moments and mid-to-late-stance hip abduction moments, smaller terminal-stance lateral GRF, and a shorter braking-phase proportion (corrected $P \leq 0.022$; $d = -0.65$ and -0.77 for AL and UL vs DL, respectively); vertical GRF was lower in the UL during terminal stance. Patellar tendon force did not differ among legs.

Conclusions: Sagittal-plane patellar tendon loading did not differ between patients with PT and controls during side-cutting, whereas bilateral frontal- and transverse-plane alterations were observed; these alterations are consistent with a dynamic rather than purely static alignment problem, although whether they precede or result from PT cannot be determined.

Rehabilitation should incorporate bilateral assessment of cutting technique and hip rotational control.

Clinical trial number: not applicable.

Keywords

biomechanics; ground reaction force; patellar tendinopathy; side-cutting; statistical parametric mapping; tendon loading

Background

Patellar tendinopathy (PT) is characterised by load-dependent pain at the inferior pole of the patella ([1]) and is an overuse injury most prevalent in sports involving repetitive jumping, such as volleyball and basketball ([2,3]). Repeated storage and release of energy in the tendon drives cumulative loading that can progressively alter tendon structure ([4,5]).

During jumping tasks, patients with PT exhibit lower-limb kinematics and kinetics that differ from those of healthy individuals, and pain-mediated unloading of the knee extensors has been reported, albeit with limited-to-moderate evidence ([6,7]). Such compensations may relieve tendon pain but increase loads elsewhere, and unilateral PT is associated with subsequent lower-extremity injury risk ([8]). Side-cutting is a common change-of-direction maneuver in team ball sports and imposes substantial knee loads ([9]), and the running cut ranks among the highest tendon-loading exercises in healthy adults ([10]). Yet biomechanical research in PT has focused on jumping and running; whether patients with PT adopt a cautious strategy during an anticipated side-cut is unknown.

The affected leg of patients with PT shows balance and control deficits relative to the unaffected leg ([11]), and unilateral tendon pain is often accompanied by contralateral deficits in muscle strength and sensory-motor function ([12,13]). Hip abductor weakness is associated with PT ([14]), and athletes with PT have weaker hip abductors and external rotators than healthy athletes ([15]), although meta-analytic evidence for modifiable risk factors remains limited ([16]). Inadequate proximal hip control may permit excessive femoral internal rotation during weight-bearing cutting, a maneuver imposing substantial frontal- and transverse-plane knee loads ([9]), although this mechanism has not been directly tested in PT.

Ground reaction force (GRF) characterises lower-limb loading during cutting, and GRF peaks have been used to phase the side-cutting maneuver ([17]). However, analyses restricted to discrete instants pre-specify the time points of interest and may miss differences elsewhere in stance. One-dimensional statistical parametric mapping (SPM) performs inference over the entire normalised waveform, identifying continuous windows of significant difference without predefined analysis windows ([18]).

This study compared the affected (AL) and unaffected (UL) legs of patients with PT and the dominant leg (DL) of healthy controls during an anticipated 45° side-cut, examining GRF waveforms, three-dimensional hip and knee angles and moments, estimated sagittal-plane patellar tendon force, and movement-strategy metrics (braking-phase proportion, hip-to-knee support moment ratio, lateral impulse share). We hypothesised that: (1) patellar tendon force would be lower in the AL than in the UL and DL; (2) the AL would exhibit greater hip internal rotation and altered frontal- and

transverse-plane knee kinematics and kinetics than the DL; and (3) these alterations would not be confined to the AL.

Materials and methods

Participants

Thirty patients with PT (PT group) and 30 healthy controls with comparable demographic characteristics (control group) were recruited between July 2023 and May 2025; all provided written informed consent. Inclusion criteria for the PT group were: (1) age 18–40 years, with regular participation in sports involving jumping and change of direction; (2) a clinical diagnosis of PT based on medical history and physical examination ([19])—gradually developed, load-dependent pain localised just inferior to the patella, with tenderness at or just distal to the inferior patellar pole; (3) pain reproduced during resisted knee extension and/or a standardised single-leg squat; and (4) a Victorian Institute of Sport Assessment–Patella (VISA-P) score ≤ 80 ([20,21]). Musculoskeletal ultrasound supported the diagnosis (tendon thickening, hypoechogenicity, and/or Doppler neovascularisation; [22]); magnetic resonance imaging (MRI) was performed when necessary to exclude other knee pathology. Controls had no history of knee injury or lower-limb surgery, normal joint range of motion, no chronic joint disorders, and no patellar tendon pathology on imaging. Exclusion criteria for both groups were trauma to other lower-limb joints, analgesic use within the past two weeks, or any other lower-limb pathology. The flow of participant selection is summarised in Figure 1.

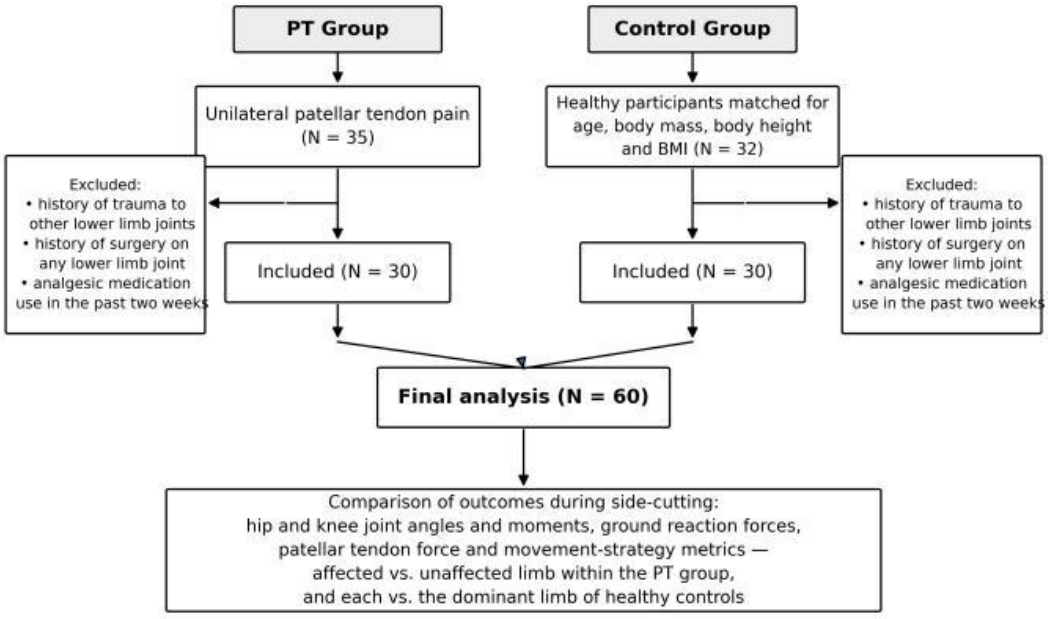


Figure 1. CONSORT flowchart of patient selection for this study. PT, patellar tendinopathy.

The sample size was estimated a priori with G*Power. The expected effect size was based on the moderate-to-large group differences in knee kinematics reported by Rosen et al. [6] in recreationally active individuals with PT (Cohen's d ranging from 0.68 for peak knee flexion to 0.97 for knee angular displacement). For the primary within-subject comparison between the affected and unaffected legs (paired-samples t-test; $\alpha = 0.05$, two-tailed; power = 0.80), 15–24 participants per group (30–48 in total) were required, depending on the effect size assumed. We therefore recruited 30 participants per group (60 in total)—matching the final sample size of Rosen et al. [6]—which also provides power ≥ 0.80 for between-group comparisons at effect sizes of $d \geq 0.74$.

Data collection

Kinematics were recorded at 100 Hz using a 12-camera infrared motion capture system (Vicon MX, Oxford Metrics, UK), and GRFs at 1000 Hz using two force platforms (AMTI BP400600), synchronised via a synchronisation box (AMTI GEN 5). A marker configuration based on the Plug-in Gait model, as used by Hao et al. [23], was applied bilaterally: anterior and posterior superior iliac spines, mid-thigh, distal lateral thigh, medial and lateral femoral condyles, proximal and distal tibia, lateral distal tibia, medial and lateral malleoli, calcaneus, and the first, second, and fifth metatarsophalangeal joints. All data collection and processing were performed by the same examiner.

Pain (Visual Analogue Scale; [24]) and VISA-P scores were recorded before testing. After a 10-minute warm-up, participants practiced the investigator-specified 45° cutting direction (Figure 2), and a static calibration trial was collected. On the command "Start", participants sprinted the 3.5-m approach at maximal speed, planted the tested leg on the second force plate, and cut at approximately 45° onto the contralateral leg. Trials were valid when approach speed was 2–3 m/s ([25]), the foot landed entirely on the plate, and data were complete; one to six valid trials per leg were retained (PT: mean 4.6; control: mean 3.3), and per-leg analyses used each participant's mean. Within-session reliability of the trial-averaged measures was good (ICC(1,k) = 0.89 for the braking-phase proportion and 0.85 for peak vertical GRF). Mean approach speed was 2.38 m/s (PT) and 2.44 m/s (control); no patient reported pain during testing.

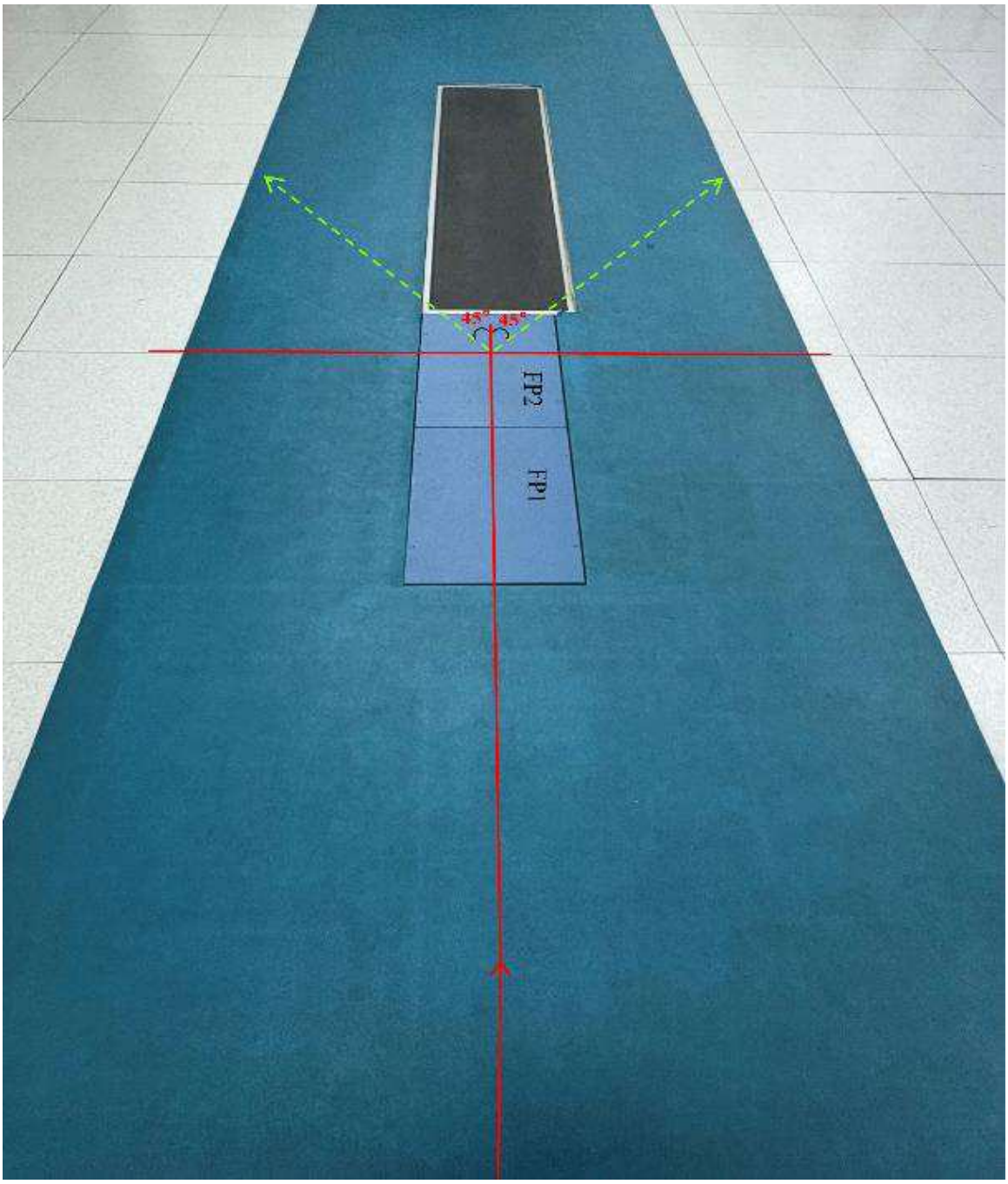
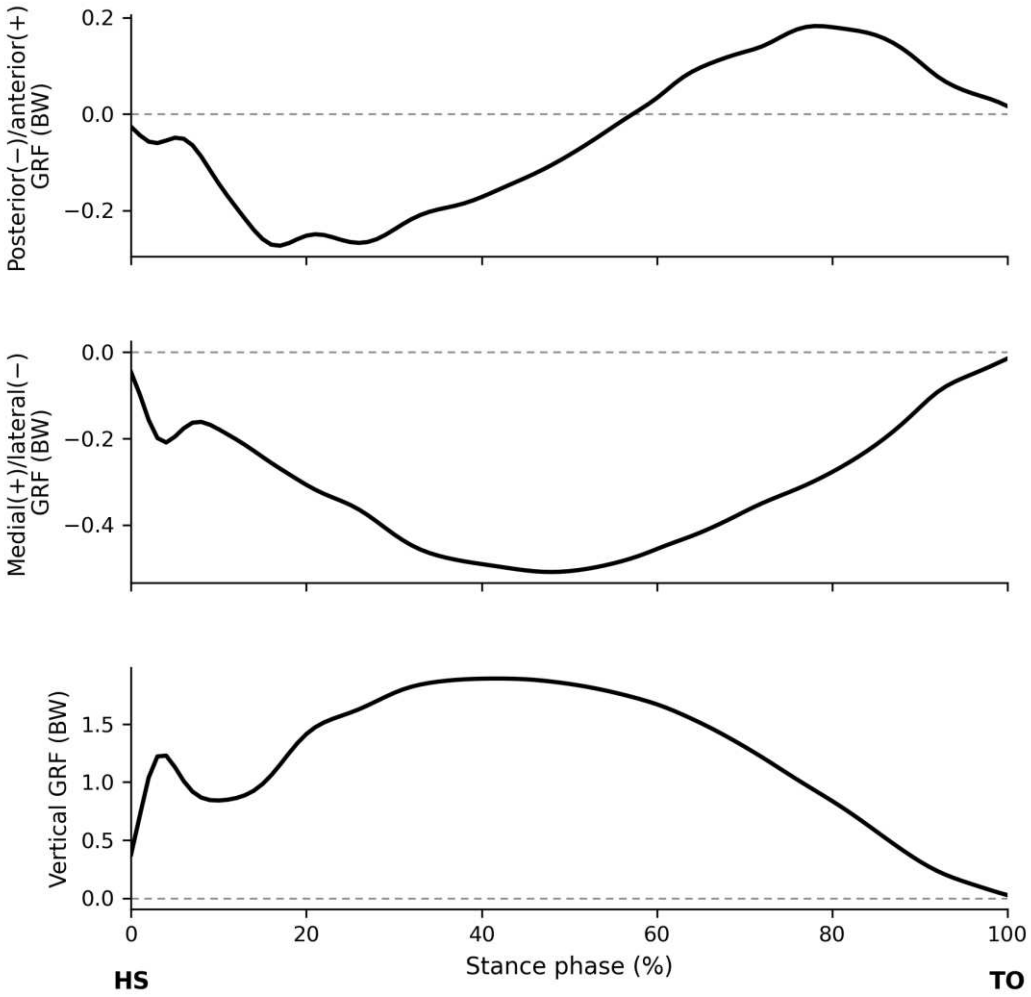


Figure 2. Schematic of the experimental setup for the 45° side-cutting task. FP1, force plate 1; FP2, force plate 2.

Data processing

Marker trajectories and GRFs were smoothed with fourth-order Butterworth low-pass filters (cut-off 10 and 200 Hz, respectively). Biomechanical modelling was performed in Visual 3D (C-Motion, Germantown, MD, USA) using a static trial with the talonavicular joint in neutral; the hip joint centre was estimated according to Bell et al. [26]. Knee angles were computed as Euler angles of the tibia relative to the femur; knee frontal-plane angles are reported as varus (+)/valgus (−). All moments are internal moments, normalised to body weight × body height (BW × BH); GRFs were normalised to body weight (BW). Stance was delimited by a 20-N vertical GRF threshold (Figure 3), and waveforms were time-normalised to 101 points (0–100% of stance) via cubic spline interpolation.



157

158 Figure 3. Representative three-component ground reaction force (GRF) waveforms during
159 the stance phase of side-cutting in one control participant (normalized to body weight,
160 BW). Anterior–posterior GRF: negative = posterior (braking), positive = anterior
161 (propulsion); mediolateral GRF: negative = lateral (toward the new direction of travel). HS:
162 heel strike; TO: toe off.

163 Three movement-strategy metrics were derived: the braking-phase proportion
164 (percentage of stance with a negative anterior–posterior GRF); the hip-to-knee support
165 moment ratio (the ratio of the stance-phase time integrals of the internal hip and knee

166 extensor moments, computed from their positive portions); and the lateral impulse share
167 (the mediolateral GRF impulse as a percentage of the total horizontal GRF impulse).

168 Sagittal-plane patellar tendon force was estimated frame by frame as the net internal
169 knee extension moment divided by the patellar tendon moment arm, an approach used in
170 landing and squatting biomechanics ([27,28]) and applied here to cutting. The moment arm,
171 normalised to leg length (greater trochanter to floor), was modeled as a function of knee
172 flexion angle φ from in vivo measurements ([29]), as implemented by Zwerver et al. [28]:
173 $\hat{d}(\varphi) = 0.022 + 0.030 \times \sin(2\varphi)$. With moments in BW × BH and leg length approximated
174 as 0.52 × body height, force is reported in BW; frames with a net internal knee flexion
175 moment were assigned zero. This approach assumes negligible knee flexor co-contraction
176 and yields a lower-bound estimate ([30]). Analyses were repeated using the moment arm
177 polynomial of Herzog and Read [31] and a constant moment arm (0.052 × leg length).

178 **Statistical analysis**

179 Outcome hierarchy and pairwise comparisons. Three pairwise leg comparisons were
180 prespecified a priori: AL versus UL (within-subject), and AL versus DL and UL versus DL
181 (between-group); the dominant leg was the leg preferred for unilateral tasks (e.g., kicking;
182 [32]). Primary outcomes were the stance-phase waveforms of hip and knee angles, internal
183 moments, GRF components, and estimated patellar tendon force, compared using one-
184 dimensional statistical parametric mapping (SPM); the three movement-strategy metrics
185 were secondary, exploratory outcomes analysed with linear mixed models (LMMs).
186 Because the three comparisons are not statistically independent, a Benjamini–Hochberg
187 false discovery rate (FDR) sensitivity analysis was performed across all supra-threshold
188 clusters ($q = 0.05$).

Statistical parametric mapping. SPM analyses were performed with the spm1d package (v0.4; www.spm1d.org; [18,33]), using paired t-tests for AL versus UL and two-sample t-tests for comparisons with the DL. Critical t thresholds ($t^* = 2.47–3.48$) were computed using random field theory at $\alpha = 0.05$ (two-tailed), with temporal smoothness estimated from the residual fields; clusters were significant when the corrected cluster-level P was < 0.05. Clusters spanning < 1% of stance at the 0% or 100% boundary were regarded as edge artifacts and not interpreted. In the FDR sensitivity analysis, every significant cluster remained significant (24 clusters identified; 16 after exclusion of boundary artifacts).

Linear mixed models. Each movement-strategy metric was analysed with an LMM, $y_{ij} = \beta_j + b_i + \varepsilon_{ij}$, with leg (AL, UL, DL) as a fixed effect and a participant-specific random intercept accounting for the within-participant correlation between a patient's two legs (intraclass correlation coefficients, 0.49–0.61); control participants contributed one observation each (DL) and were assumed independent. Models were fitted by restricted maximum likelihood; pairwise contrasts of the estimated marginal means were Bonferroni-adjusted across the three comparisons. Effect sizes are reported as Cohen's d (paired-samples dz for AL versus UL; pooled-SD d between groups). Assumptions were checked with residual diagnostics; repeating the hip-to-knee ratio analysis on log-transformed values did not change any conclusion.

Valid trials were averaged per participant and then per group in MATLAB (R2024b, MathWorks, USA); data are presented as mean ± standard deviation, and statistical significance was set at $P < 0.05$ (two-tailed) unless otherwise stated.

Results

Participant characteristics

The PT and control groups (30 participants each; 45 males and 15 females in total) did not differ in age, sex distribution, height, body mass, or body mass index ($P > 0.05$; Table 1), whereas VISA-P scores were lower in the PT group ($P < 0.001$). The affected side was the right leg in 17 patients and the left in 13; the tested dominant leg was the right in 26 controls and the left in 4. Approach speed did not differ among legs (AL 2.37 ± 0.20, UL 2.39 ± 0.24, DL 2.44 ± 0.22 m/s; all pairwise $P > 0.19$).

Table 1. Demographic characteristics of participants

Variable	PT Group, Mean (SD)	Control Group, Mean (SD)	*P* value
Sex (male/female, n)	25/5	20/10	0.136
Age (y)	27.30 (4.28)	30.40 (8.41)	0.114
Body height (cm)	176.93 (7.88)	172.28 (9.88)	0.117
Body mass (kg)	75.75 (11.48)	71.86 (15.85)	0.284
BMI (kg/m^2)	24.10 (2.60)	23.95 (3.51)	0.584
VISA-P	67.87 (8.30)	100 (0)	<0.001*

Mean, average value; SD, standard deviation; BMI, body mass index; VISA-P, Victorian Institute of Sport Assessment–Patella. PT: patellar tendinopathy.

GRF waveforms and movement-strategy metrics

Every significant supra-threshold cluster remained significant in the Benjamini–Hochberg FDR sensitivity analysis ($q = 0.05$). During terminal stance, both PT legs exhibited smaller lateral GRF than the DL (AL: 84.7–98.6% of stance, cluster $P < 0.001$; UL: 86.4–97.0%, cluster $P = 0.005$), and the UL additionally showed lower vertical GRF during 92.4–98.1% of stance (cluster $P = 0.014$; Figure 4); no clusters were detected for the anterior–posterior GRF. The braking-phase proportion was shorter in both PT legs than in the DL (AL: 56.7 ± 12.7%; UL: 56.5 ± 10.4%; DL: 63.8 ± 8.6%; AL vs DL: corrected $P = 0.022$, $d = -0.65$; UL vs DL: corrected $P = 0.018$, $d = -0.77$; AL vs UL: corrected P =

1.000; Figure 5A). The lateral impulse share did not differ among legs (approximately 68.5% in all three; all corrected P = 1.000; Figure 5B).

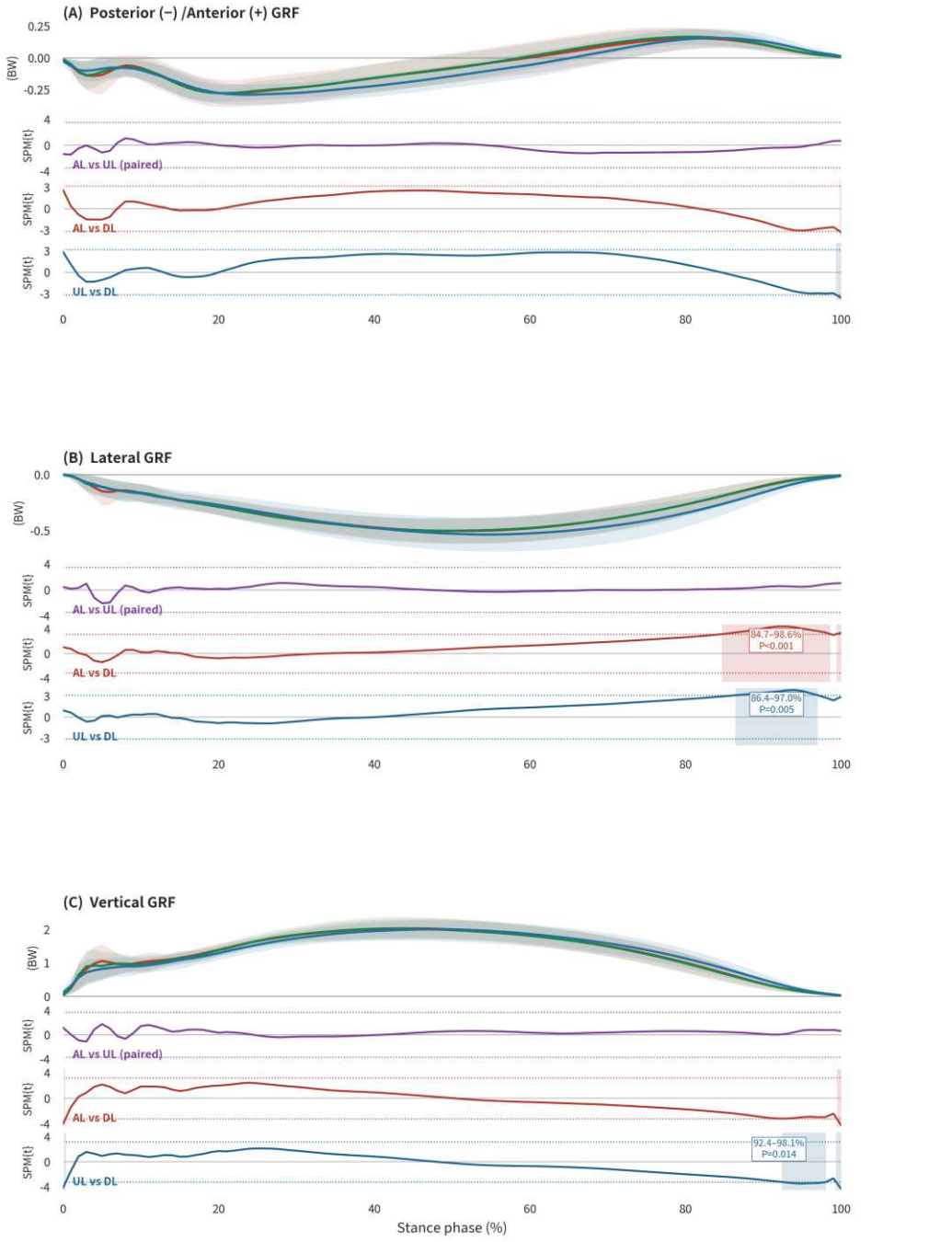


Figure 4. Anterior–posterior, lateral, and vertical ground reaction forces (normalised to body weight, BW) during the stance phase of side-cutting in both groups, with one-dimensional statistical parametric mapping (SPM) of the pairwise between-leg differences. Panels (A–C): anterior–posterior (posterior −/anterior +), lateral, and vertical GRF. In each panel, the top subplot shows group mean waveforms with shaded ±1 standard deviation bands (red line: the PT group's affected leg; green line: the PT group's unaffected leg; blue line: the control group's dominant leg; negative lateral values denote the laterally directed GRF); the three lower subplots show the SPM{t} curve of each pairwise comparison separately (top to bottom: affected vs unaffected leg, paired t-test; affected leg vs control dominant leg, two-sample t-test; unaffected leg vs control dominant leg, two-sample t-test), with dotted horizontal lines marking the random-field-theory critical thresholds ($\alpha = 0.05$, two-tailed) and shaded regions denoting significant supra-threshold clusters with cluster P values annotated; clusters confined to the immediate vicinity of touchdown or toe-off (<1% of stance) were treated as boundary artifacts and are not annotated. X-axis: normalised stance time (%).

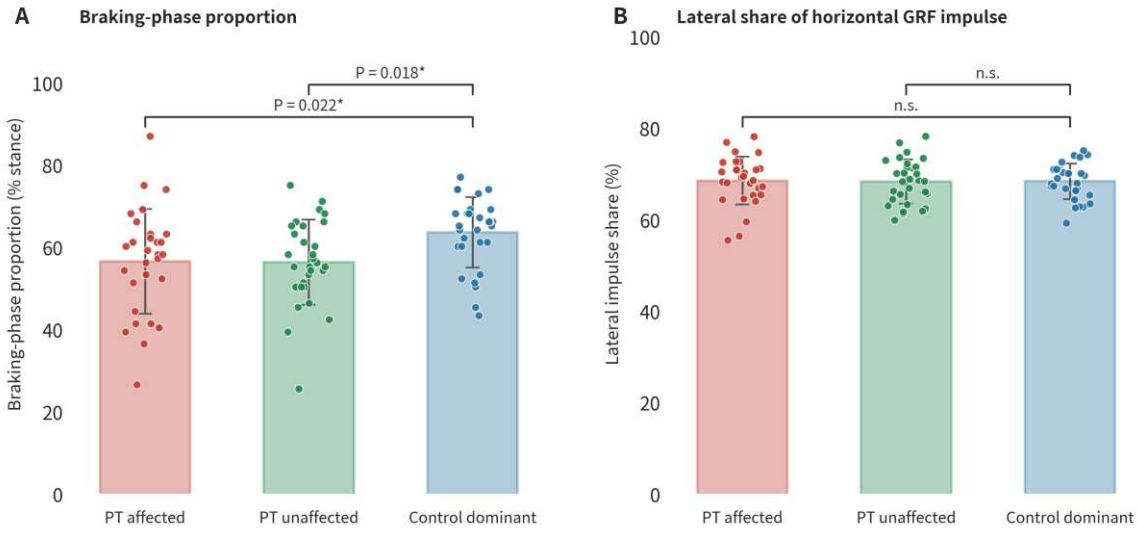


Figure 5. Ground reaction force–related movement-strategy metrics during the stance phase of side-cutting: (A) braking-phase proportion; (B) lateral impulse share. Braking-phase proportion: percentage of stance during which the anterior–posterior ground reaction force was negative (braking). Lateral impulse share: mediolateral GRF impulse as a percentage of the total horizontal GRF impulse. Bars: group means; error bars: ±1 SD; dots: individual values; brackets: Bonferroni-corrected post-hoc comparisons from linear mixed models (*P < 0.05; n.s.: not significant). AL: affected leg of patients with PT; UL: unaffected leg; DL: dominant leg of healthy controls.

Hip and knee joint angles

Significant clusters were detected for the hip internal rotation, knee varus, and knee internal/external rotation angles (Figure 6; Table 2). Versus the DL, the hip internal rotation angle was greater in the AL (0–74.8% of stance, cluster P = 0.004; 97.1–100%, cluster P = 0.050) and the UL (0–4.5%, cluster P = 0.050; 35.9–71.2%, cluster P = 0.031). Knee varus was greater in both PT legs (AL: 0–77.5%; UL: 0–89.1%; both cluster P = 0.003), and the UL showed smaller knee external rotation during 31.0–60.9% of stance (cluster P = 0.039). The AL exhibited slightly greater hip flexion than the UL during 0–10.8% of stance (cluster P = 0.046). Clusters at 0–4.5%, 0–10.8%, and 97.1–100% touched the boundaries of the analysed interval and should be interpreted with caution. No clusters were detected for the hip flexion/extension, hip abduction/adduction, or knee flexion/extension angles.

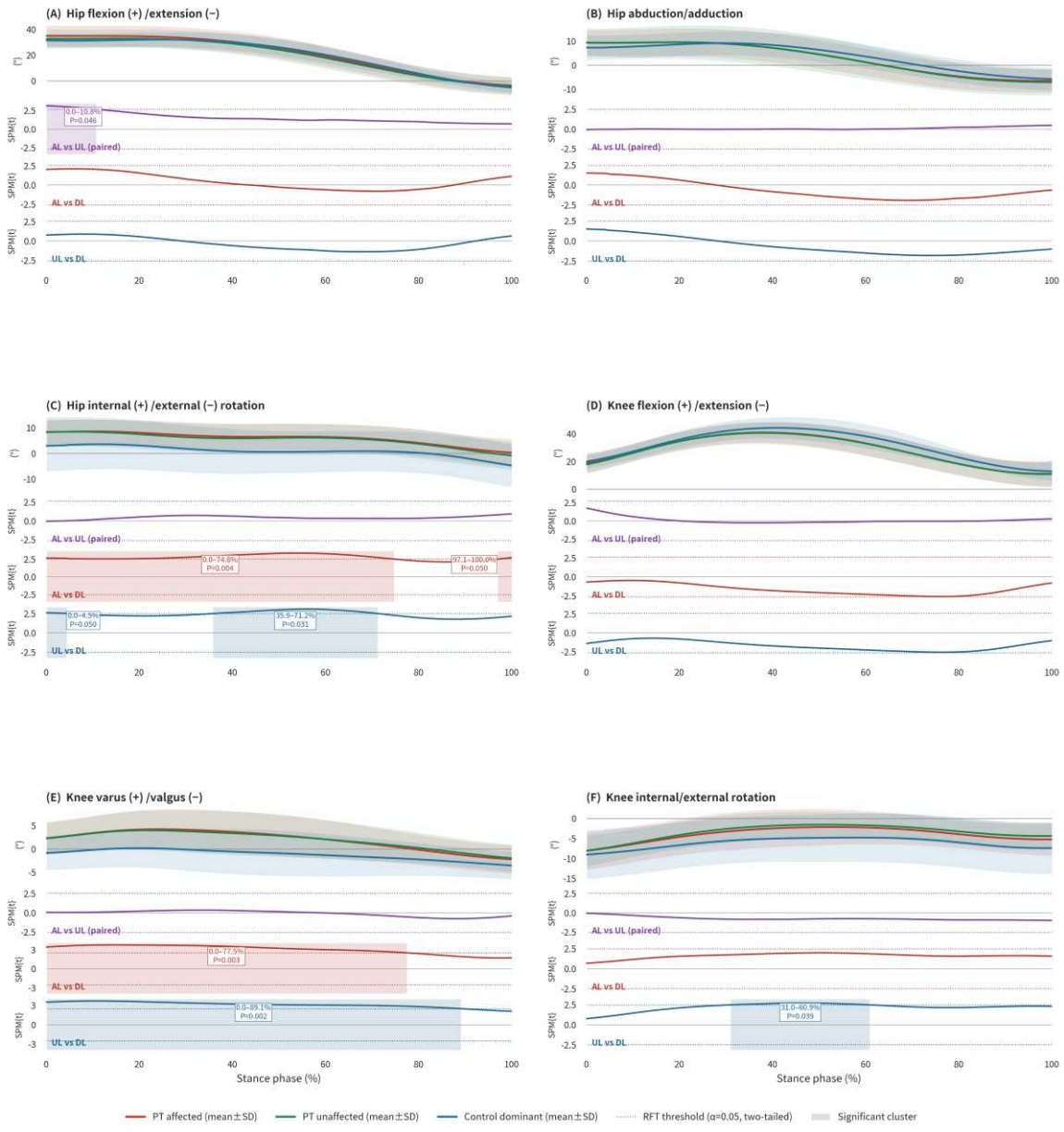


Figure 6. Hip and knee joint angles during the stance phase of side-cutting in both groups, with one-dimensional statistical parametric mapping (SPM) of the pairwise between-leg differences. Panels (A–F): hip flexion/extension, hip abduction/adduction, hip internal/external rotation, knee flexion/extension, knee varus/valgus, and knee internal/external rotation. In each panel, the top subplot shows group mean waveforms with

276 shaded ±1 standard deviation bands (red line: the PT group's affected leg; green line: the
277 PT group's unaffected leg; blue line: the control group's dominant leg); the three lower
278 subplots show the SPM{t} curve of each pairwise comparison separately (top to bottom:
279 affected vs unaffected leg, paired t-test; affected leg vs control dominant leg, two-sample t-
280 test; unaffected leg vs control dominant leg, two-sample t-test), with dotted horizontal lines
281 marking the random-field-theory critical thresholds ($\alpha = 0.05$, two-tailed) and shaded
282 regions denoting significant supra-threshold clusters with cluster P values annotated. X-
283 axis: normalised stance time (%).

284 Table 2. Group mean (SD) values within significant SPM supra-threshold windows

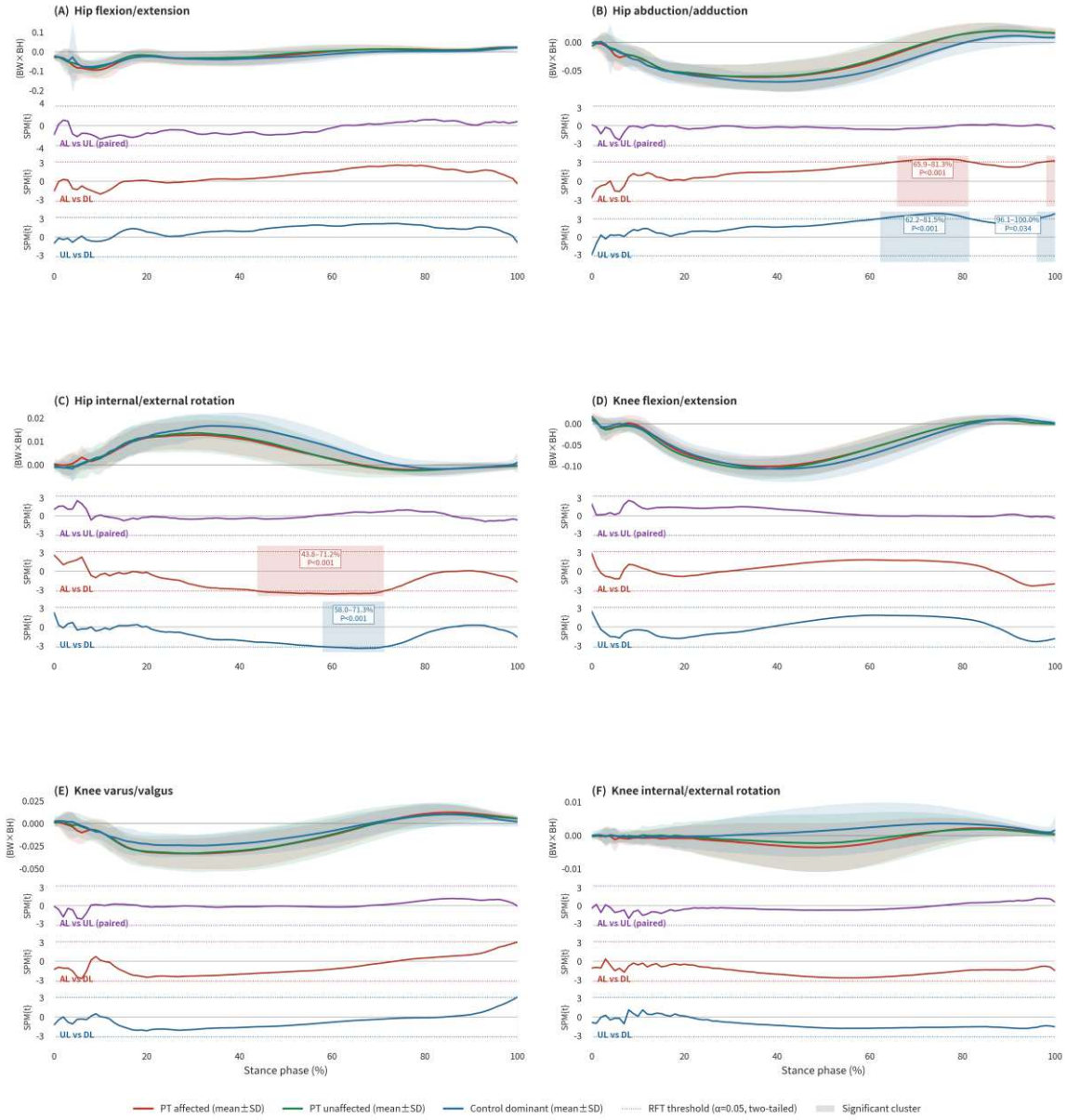
Variable	**Comparison**	**Significant window (% stance)**	**Cluster P**	**AL Mean (SD)**	**UL Mean (SD)**	**DL Mean (SD)**
Hip internal (+)/external (-) rotation angle (°)	AL vs DL	0.0–74.8	0.004	7.08 (4.54)	6.63 (5.20)	1.74 (8.61)
		97.1–100.0	0.050	0.50 (5.37)	-0.51 (5.41)	-4.28 (8.35)
	UL vs DL	0.0–4.5	0.050	8.40 (4.80)	8.41 (5.72)	3.11 (9.82)
		35.9–71.2	0.031	6.37 (4.94)	5.89 (5.38)	0.78 (8.17)
Knee varus (+)/valgus (-) angle (°)	AL vs DL	0.0–77.5	0.003	2.90 (3.93)	2.82 (3.98)	-0.72 (4.22)
	UL vs DL	0.0–89.1	0.003	2.43 (3.78)	2.41 (3.82)	-0.96 (4.07)
Knee internal (+)/external (-) rotation angle (°)	UL vs DL	31.0–60.9	0.039	-2.41 (4.50)	-1.78 (3.28)	-4.98 (5.86)
Hip flexion	AL vs UL	0.0–10.8	0.046	34.88 (8.07)	32.66 (7.32)	31.25 (5.21)

(+)/extension (-) angle (°)						
Hip adduction (+)/abduction (-) moment (BW × BH)	AL vs DL	65.9–81.3	<0.001	0.000 (0.022)	0.001 (0.020)	-0.018 (0.017)
		98.1–100.0	0.045	0.016 (0.009)	0.017 (0.007)	0.008 (0.010)
	UL vs DL	62.2–81.5	<0.001	-0.003 (0.021)	-0.003 (0.021)	-0.022 (0.017)
		96.1–100.0	0.034	0.016 (0.010)	0.017 (0.007)	0.008 (0.011)
Hip internal (+)/external (-) rotation moment (BW × BH)	AL vs DL	43.8–71.2	<0.001	0.004 (0.005)	0.004 (0.007)	0.009 (0.006)
	UL vs DL	58.0–71.3	<0.001	0.000 (0.004)	0.000 (0.005)	0.004 (0.005)
Lateral (-)/medial (+) GRF (BW)	AL vs DL	84.7–98.6	<0.001	-0.087 (0.041)	-0.090 (0.048)	-0.135 (0.052)
	UL vs DL	86.4–97.0	0.005	-0.088 (0.041)	-0.089 (0.046)	-0.134 (0.050)
Vertical GRF (BW)	UL vs DL	92.4–98.1	0.014	0.155 (0.060)	0.150 (0.058)	0.209 (0.072)

Hip and knee joint moments

Significant clusters were detected for the hip abduction/adduction and internal/external rotation moments (Figure 7; Table 2). During mid-to-late stance, when the moment acted in the abduction direction, the hip abduction moment was smaller in both PT legs than in the DL (AL: 65.9–81.3% of stance; UL: 62.2–81.5%; both cluster $P < 0.001$); during terminal stance, after the moment had reversed into the adduction direction, the hip adduction moment was larger in both PT legs (AL: 98.1–100%, cluster $P = 0.045$; UL: 96.1–100%, cluster $P = 0.034$). The hip internal rotation moment was smaller during mid-

294 stance in the AL (43.8–71.2%) and UL (58.0–71.3%; both cluster $P < 0.001$). No clusters
295 were detected for the hip flexion/extension moment or any knee moment. The hip-to-knee
296 support moment ratio did not differ among legs (AL: 0.60 ± 0.51; UL: 0.48 ± 0.38; DL:
297 0.58 ± 0.40; all corrected $P \geq 0.49$; Figure 8).



298

299 Figure 7. Hip and knee joint moments during the stance phase of side-cutting in both
300 groups, with one-dimensional statistical parametric mapping (SPM) of the pairwise

between-leg differences. Panels (A–F): hip flexion/extension, hip abduction/adduction, hip internal/external rotation, knee flexion/extension, knee varus/valgus, and knee internal/external rotation moments. In each panel, the top subplot shows group mean waveforms with shaded ±1 standard deviation bands (red line: the PT group's affected leg; green line: the PT group's unaffected leg; blue line: the control group's dominant leg); the three lower subplots show the SPM{t} curve of each pairwise comparison separately (top to bottom: affected vs unaffected leg, paired t-test; affected leg vs control dominant leg, two-sample t-test; unaffected leg vs control dominant leg, two-sample t-test), with dotted horizontal lines marking the random-field-theory critical thresholds ($\alpha = 0.05$, two-tailed) and shaded regions denoting significant supra-threshold clusters with cluster P values annotated. Moments are normalised to body weight × body height (BW × BH). X-axis: normalised stance time (%).

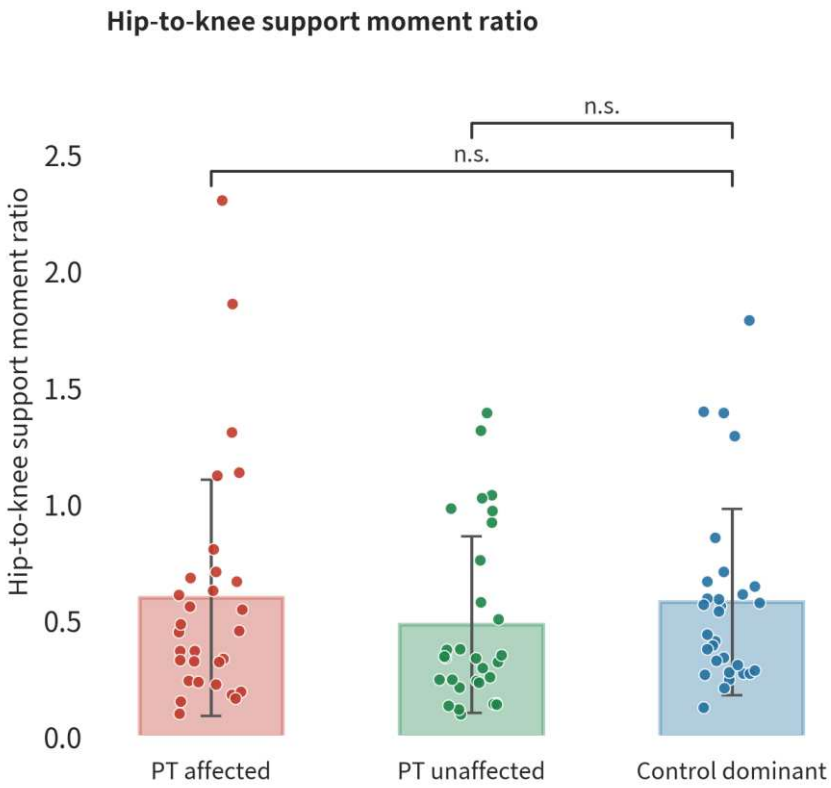


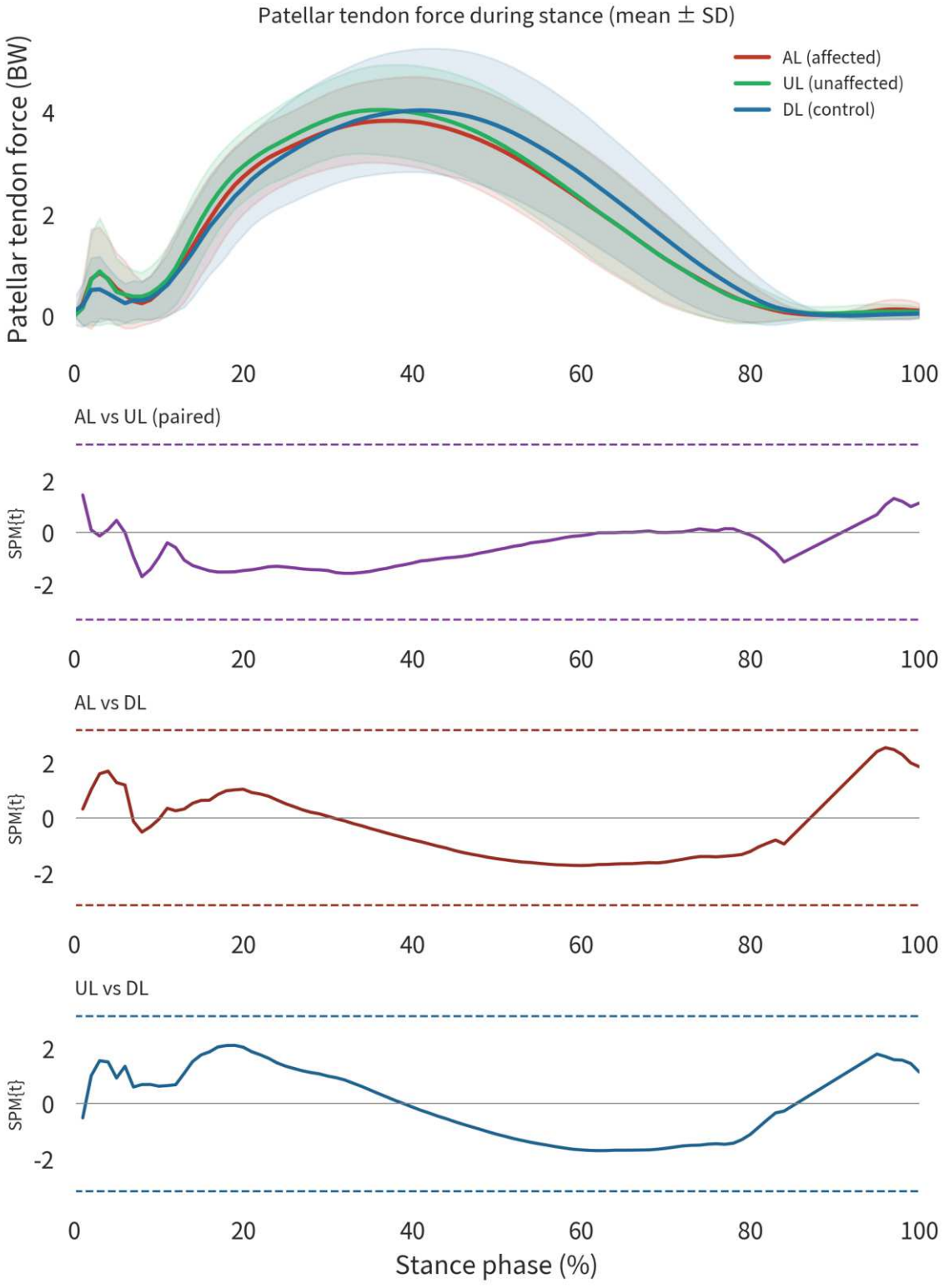
Figure 8. Hip-to-knee support moment ratio during the stance phase of side-cutting. The ratio is the stance-phase time integral of the internal hip extensor moment divided by that of the internal knee extensor moment. Bars: group means; error bars: ±1 SD; dots: individual values; brackets: Bonferroni-corrected post-hoc comparisons from linear mixed models (n.s.: not significant). AL: affected leg of patients with patellar tendinopathy; UL: unaffected leg; DL: dominant leg of healthy controls.

Values are mean (standard deviation) of the corresponding variable within each significant supra-threshold window. AL: affected leg of the PT group; UL: unaffected leg of the PT group; DL: dominant leg of healthy controls; SPM: statistical parametric mapping; Cluster

P: random-field-theory corrected P value of the supra-threshold cluster; BW × BH: body weight × body height.

Estimated patellar tendon force

SPM analysis of the patellar tendon force waveforms revealed no supra-threshold clusters in any pairwise comparison (maximum |SPM{t}| = 1.7–2.5, below the critical thresholds of 3.2–3.4; Figure 9); these null findings were unchanged across the three moment arm models.


Patellar tendon force during stance (mean ± SD)
AL (affected)
UL (unaffected)
DL (control)
Patellar tendon force (BW)
AL vs UL (paired)
AL vs DL
UL vs DL
SPM{t}
Stance phase (%)

332

Figure 9. Estimated sagittal-plane patellar tendon force (normalised to body weight, BW) during the stance phase of side-cutting in both groups, with one-dimensional statistical parametric mapping (SPM) of the pairwise between-leg differences. The top subplot shows group mean waveforms with shaded ±1 standard deviation bands (red line: the PT group's affected leg; green line: the PT group's unaffected leg; blue line: the control group's dominant leg); the three lower subplots show the SPM{t} curve of each pairwise comparison separately (top to bottom: affected vs unaffected leg, paired t-test; affected leg vs control dominant leg, two-sample t-test; unaffected leg vs control dominant leg, two-sample t-test); dotted horizontal lines: random-field-theory critical thresholds ($\alpha = 0.05$, two-tailed); no supra-threshold clusters were detected. X-axis: normalised stance time (%).

Discussion

This study combined whole-stance SPM inference with patellar tendon force estimation to compare the AL, UL, and DL during anticipated 45° side-cutting. Approach speed and cutting angle were similar between groups, and no patient reported pain; the observed differences therefore more likely reflect habitual movement strategies than acute pain-avoidance responses. Overall, patients with PT showed no reduction in sagittal-plane tendon loading, whereas between-leg differences were concentrated in frontal- and transverse-plane orientation and control.

Contrary to our first hypothesis, no supra-threshold clusters emerged for patellar tendon force, and the hip-to-knee support moment ratio showed no between-leg differences; unlike the reduced knee extensor loading reported during jumping and landing (limited-to-moderate evidence; [6,7]), no unloading strategy, distal or proximal, was detected in this

356 anticipated cutting task. A caveat: because antagonist co-contraction increases the tendon
357 force required for a given net extensor moment, any between-leg difference in co-
358 contraction would be invisible to this net-moment-based estimate. Although terminal-stance
359 GRF differed between legs, tendon force did not, consistent with the view that GRF
360 magnitude should not be used as a surrogate for tendon loading ([30])—a notion extendable
361 from landing to cutting.

362 Consistent with our second hypothesis, the affected leg exhibited the frontal- and
363 transverse-plane alterations described above, which may themselves be relevant to the
364 pathogenesis of PT. The near-stance-wide increase in hip internal rotation is plausibly
365 related to insufficient proximal hip control: hip abductor weakness has been associated with
366 PT ([14]), and athletes with PT have weaker hip abductors and external rotators than
367 healthy athletes ([15]), although meta-analytic evidence remains limited ([16]). Both PT
368 legs also exhibited greater knee varus, and the UL showed reduced knee external rotation.
369 Notably, static lower-limb alignment has no convincing association with PT ([34]); static
370 alignment was not measured here, so this contrast rests on previous literature. Increased hip
371 internal rotation can dynamically enlarge the effective Q-angle and shift the patellar tendon
372 line of action laterally, whereas greater knee varus and reduced knee external rotation
373 indicate that the extensor mechanism sustains loading outside the sagittal plane. Together,
374 these alterations raise the hypothesis that, even when the sagittal-plane load magnitude is
375 unchanged, the direction and distribution of stress within the tendon may be altered—
376 consistent with the localised proximal tendon pathology typical of PT.

377 Because jumping and landing tasks predominantly probe sagittal-plane loading, this
378 task dependence may also explain the inconsistent findings of previous jump-based studies

([7,35]), although this inference rests on cross-study comparison. Whether these alterations precede or follow the onset of PT cannot be determined cross-sectionally; prospective data from basketball players showed that pre-season landing characteristics distinguished those who later developed PT ([36]).

The shortened braking-phase proportion in both PT legs, together with the smaller terminal-stance lateral and vertical GRF, may reflect a more cautious movement strategy: patients spent a smaller share of stance decelerating and generated less laterally directed push-off force, whereas the unchanged lateral impulse share suggests that the alteration lies in the temporal structure rather than the directional mix of force application. From mid-stance onward, the hip internal rotation and abduction moments were successively attenuated, followed by reduced terminal-stance lateral GRF—a sequence consistent with a common cautious strategy expressed at different links of the kinetic chain, although temporal coupling was not formally tested. The between-leg differences in hip internal rotation and knee varus were already present from early stance (from initial contact in the AL), preceding the moment attenuation and the GRF reduction; the alignment changes were therefore not a consequence of these later kinetic changes and are consistent with an alignment pattern established early in stance. Whether they reflect altered active proximal control cannot be determined without hip strength or electromyographic data. The smaller terminal-stance lateral GRF may also contribute to the altered terminal-stance hip adduction moment through an altered resultant GRF vector orientation; however, the resultant vector was not computed directly, and these clusters spanned only 1.9–3.9% of stance and should be considered preliminary.

Consistent with our third hypothesis, the alterations were not confined to the AL: the UL differed from the DL in knee varus, hip internal rotation, knee external rotation, and hip moments, and differed from the AL only in a slightly smaller hip flexion angle during early stance (approximately 2°; a boundary-touching cluster to be interpreted with caution). PT is therefore associated with bilateral biomechanical changes, in the sense that each PT leg differed from the control dominant leg; because limb dominance was not recorded in the PT group, this interpretation awaits confirmation in dominance-matched studies. This bilateral pattern is consistent with evidence that unilateral tendon pain is accompanied by bilateral sensory and motor deficits ([13], predominantly in lateral epicondylalgia), with reports of bilateral isokinetic knee-strength deficits in patients with PT ([12]), and with altered landing kinematics in PT groups ([6]; for conflicting systematic-review evidence, see Tayfur et al., 2022). In professional volleyball players with PT, knee extensor strength was reduced bilaterally despite symmetric jump performance ([12]). The mechanisms remain unclear; central nervous system adaptations ([37]) and cross-education effects documented in healthy individuals ([38]) are possible explanations, although neither can be confirmed here. The approximately 2° hip flexion difference was not accompanied by detectable differences in hip moments or tendon force; a protective load redistribution toward the affected side therefore cannot be inferred from this postural difference alone.

These findings carry practical implications. Progressive sagittal-plane tendon loading is recommended as an initial conservative treatment for PT and outperforms alternative protocols ([20]), and our results suggest that this approach targets a load magnitude that patients already maintain during cutting. For athletes returning to change-of-direction sports, rehabilitation and return-to-sport assessment should additionally

incorporate cutting-technique evaluation and training targeting hip rotational control and dynamic knee alignment, and bilateral involvement suggests that both legs may need to be addressed, although this requires interventional testing. To our knowledge, this is the first study to characterise three-dimensional hip and knee biomechanics and estimated patellar tendon force during side-cutting in PT; the findings are consistent with reframing the malalignment hypothesis ([34]) as a dynamic, possibly task-specific phenomenon rather than a purely static deficit.

Strengths and limitations

Strengths of this study include the whole-stance SPM analysis, which avoids pre-specified analysis windows, and the use of LMMs accounting for the within-subject correlation between legs. Several limitations should be noted. First, the cross-sectional design precludes causal inference. Second, hip muscle strength and activation were not assessed, so the proposed proximal-control mechanisms remain inferential. Third, ankle biomechanics were not analysed, although ankle position can influence knee extensor moment demand. Fourth, no neurophysiological assessment was conducted. Fifth, covariate-adjusted analyses were not performed; although the groups were demographically comparable, residual confounding of between-group comparisons cannot be excluded. Sixth, limb dominance was not recorded in the PT group; although the affected side was nearly evenly distributed (17 right, 13 left) and both PT legs showed parallel alterations, an influence of dominance cannot be excluded. Seventh, several clusters touched the boundaries of the analysed interval. Eighth, patellar tendon force was estimated with a simplified sagittal-plane model assuming negligible flexor co-contraction—a lower-bound estimate that cannot capture non-sagittal loading or tendon stress. Ninth, symptom duration,

sport discipline, and treatment history were not recorded; the VISA-P scores (mean 67.9/100) and absence of pain during testing indicate a low-symptom sample. Tenth, the anticipated task may not generalise to unanticipated, game-like cutting ([39]). Longitudinal studies combining strength, electromyographic, and neurophysiological measures are warranted.

Conclusions

During anticipated side-cutting, patients with PT exhibited increased hip internal rotation and knee varus spanning most of stance, reduced knee external rotation during mid-stance in the unaffected leg, attenuated hip internal rotation and abduction moments, smaller terminal-stance lateral GRF, and a shortened braking phase—in both legs—while approach speed and estimated sagittal-plane patellar tendon force remained similar to those of healthy controls. PT was thus associated with dynamic, bilateral alterations in alignment and control—both the affected and unaffected legs differed from the control dominant leg—rather than a purely unilateral pattern. Because static alignment was not measured and only side-cutting was tested, a dynamic, possibly task-specific mechanism is suggested but static contributions cannot be ruled out; the underlying mechanisms remain speculative, and the sagittal-plane tendon force estimate cannot capture non-sagittal loading. Whether these alterations precede or result from PT cannot be determined cross-sectionally. Side-cutting assessment may help identify altered movement patterns, and rehabilitation may need to consider bilateral training of hip control and dynamic knee alignment.

Abbreviations

AL: affected leg; BH: body height; BW: body weight; DL: dominant leg; FDR: false discovery rate; GRF: ground reaction force; ICC: intraclass correlation coefficient; LMM:

linear mixed model; MD: mean difference; MRI: magnetic resonance imaging; PT: patellar tendinopathy; SD: standard deviation; SPM: statistical parametric mapping; UL: unaffected leg; VISA-P: Victorian Institute of Sport Assessment–Patella questionnaire

Declarations

Ethics approval and consent to participate: The study was approved by the Medical Science Research Ethics Committee of Peking University Third Hospital (approval No. M2024097) and conducted in accordance with the Declaration of Helsinki. Written informed consent was obtained from all participants.

Consent for publication: Not applicable.

Competing interests: The authors declare that they have no competing interests.

Availability of data and materials: The datasets generated and analysed during the current study are available from the corresponding author upon reasonable request.

Funding: This work was partially supported by the Peking University Third Hospital Fund for Interdisciplinary Research (BYSYJC2025059) and the Clinical Key Projects of Peking University Third Hospital (BYSYZD2025014). The funders had no role in study design, data collection, analysis and interpretation, writing of the report, or the decision to submit the article for publication.

Authors' contributions: QQW and LJC conceived and designed the study, collected and curated the data, and drafted the manuscript. YJZ and SZ performed the formal analysis. SR and HSH supervised the study and revised the manuscript critically. All authors read and approved the final manuscript.

Acknowledgements: Not applicable. During the preparation of this work, the authors used generative artificial intelligence tools (Kimi, Moonshot AI; Qwen, Alibaba) for language editing and text revision. After using these tools, the authors reviewed and edited the content as needed and take full responsibility for the content of the publication.

References

1. Aicale R, Oliviero A, Maffulli N. Management of Achilles and patellar tendinopathy: What we know, what we can do. Journal of Foot and Ankle Research. 2020;13(1):59. https://doi.org/10.1186/s13047-020-00418-8

2. Lian OB, Engebretsen L, Bahr R. Prevalence of jumper's knee among elite athletes from different sports: A cross-sectional study. The American Journal of Sports Medicine. 2005;33(4):561–567. https://doi.org/10.1177/0363546504270454

3. Zwerver J, Bredeweg SW, van den Akker-Scheek I. Prevalence of jumper's knee among nonelite athletes from different sports: A cross-sectional survey. The American Journal of Sports Medicine. 2011;39(9):1984–1988.

4. Cook JL, Purdam CR. Is tendon pathology a continuum? A pathology model to explain the clinical presentation of load-induced tendinopathy. British Journal of Sports Medicine. 2009;43(6):409–416. https://doi.org/10.1136/bjsm.2008.051193

5. Magnusson SP, Langberg H, Kjaer M. The pathogenesis of tendinopathy: Balancing the response to loading. Nature Reviews Rheumatology. 2010;6(5):262–268. https://doi.org/10.1038/nrrheum.2010.43

6. Rosen AB, Ko J, Simpson KJ, Kim SH, Brown CN. Lower extremity kinematics during a drop jump in individuals with patellar tendinopathy. Orthopaedic Journal of

Sports Medicine. 2015;3(3):2325967115576100. https://doi.org/10.1177/2325967115576100

7. Tayfur A, Haque A, Salles JI, Malliaras P, Screen H, Morrissey D. Are landing patterns in jumping athletes associated with patellar tendinopathy? A systematic review with evidence gap map and meta-analysis. Sports Medicine. 2022;52(1):123–137. https://doi.org/10.1007/s40279-021-01550-6

8. Fendri T, Rebai H, Harrabi MA, Chaari F, Boyas S, Beaune B, Sahli S. Athletes with unilateral patellar tendinopathy have increased subsequent lower extremity musculoskeletal injury risk. European Journal of Sport Science. 2022;22(12):1908–1915. https://doi.org/10.1080/17461391.2021.1976840

9. Besier TF, Lloyd DG, Cochrane JL, Ackland TR. External loading of the knee joint during running and cutting maneuvers. Medicine & Science in Sports & Exercise. 2001;33(7):1168–1175. https://doi.org/10.1097/00005768-200107000-00014

10. Scattone Silva R, Song KE, Hullfish TJ, Sprague AL, Silbernagel KG, Baxter JR. Patellar tendon load progression during rehabilitation exercises: Implications for the treatment of patellar tendon injuries. Medicine & Science in Sports & Exercise. 2024;56(3):545–552. https://doi.org/10.1249/mss.0000000000003323

11. Fendri T, Boyas S, Sahli S, Harrabi MA, Chaari F, Rebai H, Beaune B. Patellar tendinopathy impairs postural control in athletes: A case-control study. Physical Therapy in Sport. 2022;53:14–20. https://doi.org/10.1016/j.ptsp.2021.10.014

12. Chantrelle M, Menu P, Gernigon M, Louguet B, Dauty M, Fouasson-Chailloux A. Consequences of patellar tendinopathy on isokinetic knee strength and jumps in

professional volleyball players. Sensors. 2022;22(9):3590. https://doi.org/10.3390/s22093590

13. Heales LJ, Lim ECW, Hodges PW, Vicenzino B. Sensory and motor deficits exist on the non-injured side of patients with unilateral tendon pain and disability—implications for central nervous system involvement: A systematic review with meta-analysis. British Journal of Sports Medicine. 2014;48(19):1400–1406. https://doi.org/10.1136/bjsports-2013-092535

14. Mendonça LD, Ocarino JM, Bittencourt NFN, Macedo LG, Fonseca ST. Association of hip and foot factors with patellar tendinopathy (jumper's knee) in athletes. Journal of Orthopaedic & Sports Physical Therapy. 2018;48(9):676–684. https://doi.org/10.2519/jospt.2018.7426

15. Zhang ZJ, Lee WC, Ng GYF, Fu SN. Isometric strength of the hip abductors and external rotators in athletes with and without patellar tendinopathy. European Journal of Applied Physiology. 2018;118(8):1635–1640. https://doi.org/10.1007/s00421-018-3896-x

16. Sprague AL, Smith AH, Knox P, Pohlig RT, Grävare Silbernagel K. Modifiable risk factors for patellar tendinopathy in athletes: A systematic review and meta-analysis. British Journal of Sports Medicine. 2018;52(24):1575–1585. https://doi.org/10.1136/bjsports-2017-099000

17. Gao M, Ge X, Tao Y, Suo L, Ren S, Ao Y. Biomechanical compensation patterns across different phases of side-cutting following anterior cruciate ligament

559 reconstruction. Bioengineering. 2025;12(12):1280.
560 https://doi.org/10.3390/bioengineering12121280
561 18. Pataky TC, Vanrenterghem J, Robinson MA. Zero- vs. one-dimensional, parametric vs.
562 non-parametric, and confidence interval vs. hypothesis testing procedures in one-
563 dimensional biomechanical trajectory analysis. Journal of Biomechanics.
564 2015;48(7):1277–1285. https://doi.org/10.1016/j.jbiomech.2015.02.051
565 19. Maffulli N, Oliva F, Loppini M, Aicale R, Spiezia F, King JB. The Royal London
566 Hospital Test for the clinical diagnosis of patellar tendinopathy. Muscles,
567 Ligaments and Tendons Journal. 2017;7(2):315–322.
568 https://doi.org/10.11138/mltj/2017.7.2.315
569 20. Breda SJ, Oei EHG, Zwerver J, Visser E, Waarsing E, Krestin GP, de Vos RJ.
570 Effectiveness of progressive tendon-loading exercise therapy in patients with
571 patellar tendinopathy: A randomised clinical trial. British Journal of Sports
572 Medicine. 2021;55(9):501–509. https://doi.org/10.1136/bjsports-2020-103403
573 21. Visentini PJ, Khan KM, Cook JL, Kiss ZS, Harcourt PR, Wark JD. The VISA score:
574 An index of severity of symptoms in patients with jumper's knee (patellar
575 tendinosis). Journal of Science and Medicine in Sport. 1998;1(1):22–28.
576 https://doi.org/10.1016/s1440-2440(98)80005-4
577 22. Warden SJ, Kiss ZS, Malara FA, Ooi ABT, Cook JL, Crossley KM. Comparative
578 accuracy of magnetic resonance imaging and ultrasonography in confirming
579 clinically diagnosed patellar tendinopathy. The American Journal of Sports
580 Medicine. 2007;35(3):427–436. https://doi.org/10.1177/0363546506294858

581 23. Hao Y, Ren S, Zhu Y, He TC, Miao X, Xu Y. Three-dimensional lower limb
582 kinematics and kinetics in femoroacetabular impingement syndrome (FAIS) patients
583 with and without borderline developmental dysplasia of the hip (BDDH) during
584 level walking. BMC Musculoskeletal Disorders. 2025;26(1):488.
585 https://doi.org/10.1186/s12891-025-08727-4
586
587 24. Hawker GA, Mian S, Kendzerska T, French M. Measures of adult pain: Visual Analog
588 Scale for Pain (VAS Pain), Numeric Rating Scale for Pain (NRS Pain), McGill Pain
589 Questionnaire (MPQ), Short-Form McGill Pain Questionnaire (SF-MPQ), Chronic
590 Pain Grade Scale (CPGS), Short Form-36 Bodily Pain Scale (SF-36 BPS), and
591 Measure of Intermittent and Constant Osteoarthritis Pain (ICOAP). Arthritis Care &
592 Research. 2011;63(S11):S240–S252. https://doi.org/10.1002/acr.20543
593 25. Xie D, Urabe Y, Ochiai J, Kobayashi E, Maeda N. Sidestep cutting maneuvers in
594 female basketball players: Stop phase poses greater risk for anterior cruciate
595 ligament injury. The Knee. 2013;20(2):85–89.
596 https://doi.org/10.1016/j.knee.2012.07.003
597 26. Bell AL, Pedersen DR, Brand RA. A comparison of the accuracy of several hip center
598 location prediction methods. Journal of Biomechanics. 1990;23(6):617–621.
599 https://doi.org/10.1016/0021-9290(90)90054-7
600 27. Edwards S, Steele JR, Purdam CR, Cook JL, McGhee DE. Alterations to landing
601 technique and patellar tendon loading in response to fatigue. Medicine & Science in
602 Sports & Exercise. 2014;46(2):330–340.
603 https://doi.org/10.1249/mss.0b013e3182a42e8e

28. Zwerver J, Bredeweg SW, Hof AL. Biomechanical analysis of the single-leg decline squat. British Journal of Sports Medicine. 2007;41(4):264–268. https://doi.org/10.1136/bjsm.2006.032482

29. Krevolin JL, Pandy MG, Pearce JC. Moment arm of the patellar tendon in the human knee. Journal of Biomechanics. 2004;37(5):785–788. https://doi.org/10.1016/j.jbiomech.2003.09.010

30. Edwards S, Steele JR, Cook JL, Purdam CR, McGhee DE, Munro BJ. Characterizing patellar tendon loading during the landing phases of a stop-jump task. Scandinavian Journal of Medicine & Science in Sports. 2012;22(1):2–11. https://doi.org/10.1111/j.1600-0838.2010.01119.x

31. Herzog W, Read LJ. Lines of action and moment arms of the major force-carrying structures crossing the human knee joint. Journal of Anatomy. 1993;182(Pt 2):213–230.

32. Shi H, Ren S, Huang H, Liu H, Liang Z, Yu Y, Li H, Ao Y. Bilateral alterations in isokinetic strength and knee biomechanics during side-cutting 1 year after unilateral ACL reconstruction. The American Journal of Sports Medicine. 2022;50(11):2961–2971. https://doi.org/10.1177/03635465221112940

33. Pataky TC. One-dimensional statistical parametric mapping in Python. Computer Methods in Biomechanics and Biomedical Engineering. 2012;15(3):295–301. https://doi.org/10.1080/10255842.2010.527837

34. van der Worp H, van Ark M, Roerink S, Pepping GJ, van den Akker-Scheek I, Zwerver J. Risk factors for patellar tendinopathy: A systematic review of the literature.

British Journal of Sports Medicine. 2011;45(5):446–452. https://doi.org/10.1136/bjsm.2011.084079

35. Ben Zaki B, Julia M, Desmyttere G, Perrey S, Dusfour G. Altered landing strategy during vertical jump tasks in elite volleyball players with patellar tendinopathy. Physical Therapy in Sport. 2025;74:96–103. https://doi.org/10.1016/j.ptsp.2025.05.011

36. Feng R, Best TM, Wang L, Gao W, Liu H, Yu B. Knee movement characteristics of basketball players in landing tasks before onset of patellar tendinopathy: A prospective study. Frontiers in Sports and Active Living. 2022;4:847945. https://doi.org/10.3389/fspor.2022.847945

37. Rio E, Kidgell D, Moseley GL, Gaida J, Docking S, Purdam C, Cook J. Tendon neuroplastic training: Changing the way we think about tendon rehabilitation: A narrative review. British Journal of Sports Medicine. 2016;50(4):209–215. https://doi.org/10.1136/bjsports-2015-095215

38. Colomer-Poveda D, Romero-Arenas S, Keller M, Hortobágyi T, Márquez G. Effects of acute and chronic unilateral resistance training variables on ipsilateral motor cortical excitability and cross-education: A systematic review. Physical Therapy in Sport. 2019;40:143–152. https://doi.org/10.1016/j.ptsp.2019.09.006

39. Okamura K, Uehara S, Kanai S. Lower-extremity kinematics during unanticipated side-cutting including before initial ground contact. Gait & Posture. 2026;124:110050. https://doi.org/10.1016/j.gaitpost.2025.110050

649

650

651

652

653

654

655

656

657

658

659